

RESEARCH ARTICLE

Confirmation of Specific Binding of the 18-kDa Translocator Protein (TSPO) Radioligand [¹⁸F]GE-180: a Blocking Study Using XBD173 in Multiple Sclerosis Normal Appearing White and Grey Matter

Sujata Sridharan¹,¹ Joel Raffel,¹ Ashwini Nandoskar,¹ Chris Record,¹ David J. Brooks,^{1,2,3} David Owen,¹ David Sharp,¹ Paolo A. Muraro,¹ Roger Gunn,⁴ Richard Nicholas¹

¹Division of Brain Sciences, Faculty of Medicine, Imperial College London, Hammersmith Hospital Campus, Burlington Danes Building, Du Cane Road, London, W12 0NN, UK

²Institute of Clinical Medicine, Aarhus University, Aarhus, Denmark

³Institute of Neuroscience, Newcastle upon Tyne University, Newcastle upon Tyne, UK

⁴Invicro Ltd., London, UK

Abstract

Purpose: Measurements of non-displaceable binding (V_{ND}) of positron emission tomography (PET) ligands are not often made *in vivo* in humans because they require ligands to displace binding to target receptors and there are few readily available, safe ones to use. A technique to measure V_{ND} for ligands for the 18-kDa translocator protein (TSPO) has recently been developed which compares the total volume of distribution (V_T) before and after administration of the TSPO ligand XBD173. Here, we used XBD173 with an occupancy plot to quantify V_{ND} for two TSPO radiotracers, [¹⁸F]GE-180 and [¹¹C]PBR28, in cohorts of people with multiple sclerosis (MS). Additionally, we compared plots of subjects carrying high (HAB) or mixed binding (MAB) affinity polymorphisms of TSPO to estimate V_{ND} without receptor blockade.

Procedures: Twelve people with MS underwent baseline MRI and 90-min dynamic [¹⁸F]GE-180 PET or [¹¹C]PBR28 PET ($n=6$; three HAB, three MAB each). Arterial blood sampling was used to generate plasma input functions for the two-tissue compartment model. V_{ND} was calculated using two independent methods: the occupancy plot (by modelling the differences in signal post XBD173) and the polymorphism plot (by modelling the differences in signal across presence and absence of rs6971 genotypes).

Results: Whole brain V_T (mean \pm standard deviation) was 0.29 ± 0.17 ml/cm³ for [¹⁸F]GE-180 and 5.01 ± 1.88 ml/cm³ for [¹¹C]PBR28. Using the occupancy and polymorphism plots respectively, V_{ND} for [¹⁸F]GE-180 was 0.11 ml/cm³ (95 % CI = 0.02, 0.16) and 0.20 ml/cm³ (0.16, 0.34), accounting for, on average, 55 % of V_T in the whole brain. For [¹¹C]PBR28, these values were 3.81 ml/cm³ (3.02, 4.21) and 3.49 ml/cm³ (1.38, 4.27), accounting for 67 % of average whole brain V_T .

Sujata Sridharan and Joel Raffel are joint first authors.

Correspondence to: Sujata Sridharan; e-mail: s.sridharan@imperial.ac.uk

Conclusions: Although V_T for [¹⁸F]GE-180 is low, indicating low brain penetration, half the signal shown by MS subjects reflected specific TSPO binding. V_T for [¹¹C]PBR28 was higher and two thirds of the binding was non-specific. No brain ROIs were devoid of specific signal, further confirming that true reference tissue approaches are potentially problematic for estimating TSPO levels.

Key words: PET, Occupancy plot, Polymorphism plot, Multiple sclerosis, [¹⁸F]GE-180, [¹¹C]PBR28, XBD173

Introduction

Several positron emission tomography (PET) ligands exist for the 18-kDa translocator protein (TSPO), which can be upregulated in the mitochondria of activated microglia when the central nervous system becomes inflamed (see [1] for review). Currently, it is unclear, in humans, what proportion of the observed *in vivo* PET signal represents specific TSPO binding and what proportion is merely non-displaceable binding. This is a particular problem with TSPO imaging as (1) the binding of a large majority of TSPO ligands is affected by carriage of a single nucleotide polymorphism (SNP rs6971) and (2) affinity thus varies according to whether participants are homozygotic (high or low affinity binders, HABs/LABs) or heterozygotic (mixed affinity binders, MABs). This results in increased tracer-specific variability across cohorts [2]. TSPO is known to be expressed ubiquitously throughout the human brain, meaning that there is no suitable reference region (free of specific binding) which would allow the non-displaceable proportion of the signal to be estimated *in vivo* (see [3] for overview). Assuming that the fraction of non-displaceable binding is negligible can dramatically affect the interpretation of results. It is therefore important to investigate the proportion of binding that is specific for each TSPO tracer [4, 5].

Approaches recently described by Owen et al. [6] and Guo et al. [7] can be used to estimate the non-displaceable component of the total volume of distribution (V_{ND}) *in vivo*. In short, for the TSPO ligand of interest, the total volume of distribution, V_T , is calculated both before and after blockade with the TSPO ligand XBD173. V_{ND} is derived from the x -intercept of the graph of $V_T^{baseline}$ against $V_T^{baseline} - V_T^{block}$ (see ‘Materials and Methods’). In addition, use of a polymorphism plot (Guo, et al. [8]), which assumes that MABs express an equal percentage of high and low affinity binding sites [6, 9], allows V_{ND} to be derived from the x -intercept of V_T^{HAB} against $V_T^{HAB} - V_T^{MAB}$ (see ‘Materials and Methods’).

One recently developed ligand, [¹⁸F]GE-180, has exhibited a higher signal to background ratio than (R)-[¹¹C]PK11195 in several preclinical models [10–12]. However, in human studies, it has shown unexpectedly low brain penetration [13–15]. Additionally, *in vitro* data shows that binding of [¹⁸F]GE-180 to TSPO is sensitive

to the presence of the rs6971 SNP [2, 9, 16]; however, in these *in vivo* human studies, the expected genotype dependence of signals was not observed [13, 14]. This phenomenon may be due to poor extraction of [¹⁸F]GE-180 over the blood–brain barrier (BBB) and/or the action of active efflux pumps such as P-glycoprotein. Given these unexpected results, we wished to clarify the proportion of [¹⁸F]GE-180 uptake detected with PET in the human brain that is non-displaceable. A recent blocking study in healthy control subjects confirmed the presence of specific binding throughout the human brain with [¹¹C]PBR28 [6]. Here, we describe a similar blocking study to investigate whether (and what proportion of) [¹⁸F]GE-180 and [¹¹C]PBR28 PET signal is specific to TSPO binding in people with multiple sclerosis (MS).

Materials and Methods

Participants

Twelve people with clinically definite MS according to revised 2010 MacDonald criteria were recruited from the Imperial College Healthcare NHS Trust. The participants were aged between 20 and 50 years old and provided written informed consent, under ethics reviewed by the London Riverside Research Ethics Committee (REC reference 14/LO/0343 [¹⁸F]GE-180-scanned participants, 13/LO/1916 [¹¹C]PBR28-scanned participants).

Participants attended a screening visit, including clinical ratings with the expanded disability status scale (EDSS) [17] and the collection of blood, to establish TSPO SNP genotype. Predicted LABs were excluded. Participants returned for a baseline visit where they underwent MRI and a 90-min dynamic [¹⁸F]GE-180 or [¹¹C]PBR28 PET scan. One week later [¹⁸F]GE-180, or on the afternoon of the same day [¹¹C]PBR28, participants returned for a ‘post-blockade’ scan; they were administered a 90-mg oral dose of XBD173 2 h prior to a repeat PET scan with the same tracer and dose as previously administered. The dose of 90 mg was selected based on that previously calculated by Owen et al. in a blocking study using [¹¹C]PBR28 to achieve at least 75 % XBD173 occupancy in adult participants [6].

Arterial Plasma Measurement

Participants had radial artery cannulation and blood was withdrawn continuously at a target rate of 2.5 ml min⁻¹ from the start of each scan for the first 15 min. In addition, discrete blood samples were drawn at 0, 5, 10, 15, 30, 50, 70 and 90 min ([¹⁸F]GE-180) or 0, 5, 10, 15, 20, 25, 30, 40, 50, 60, 70, 80 and 90 min ([¹¹C]PBR28) for metabolite analysis. For [¹⁸F]GE-180, tracer concentrations in whole blood and plasma were measured in a well counter and radiometabolite analysis performed using two high performance liquid chromatography (HPLC) systems (Agilent 1260 Infinity and Agilent 110 Series) in isocratic mode. Briefly, samples were spun down to obtain plasma, which was then added to HPLC-grade acetonitrile to precipitate proteins. After centrifugation, the samples were rotary evaporated and analytes collected and reconstituted in 7 % ethanol solution and filtered in 15-mm syringe filters with a nylon membrane of pore size 0.2 μm. For [¹¹C]PBR28, methods described by Owen et al. [6] were used to determine the parent fraction of tracer in plasma and whole blood.

Scanning Protocol

All participants scanned with [¹⁸F]GE-180 underwent MR scans on a 3-T Siemens Magnetom MR B19 scanner, including T1 magnetisation prepared rapid gradient echo (MPRAGE) sequences. [¹⁸F]GE-180 was synthesised, as previously described, on a FastLab™ platform [18]. A low-dose CT scan was performed for attenuation correction immediately prior to a 90-min dynamic PET scan on a Siemens Biograph 6 with a field of view of 168 × 168 × 148 mm³. The tracer was injected as an intravenous bolus over the course of 30 s with a target dose of 185 MBq. List-mode data were histogrammed into 24 frames (6 × 15 s, 3 × 60 s, 5 × 120 s, 5 × 300 s and 5 × 600 s) and reconstructed using filtered back projection (FBP) with a ramp filter. Reconstructed voxel size and spatial resolution were 1.57 × 1.57 × 1.92 and ~5 mm, respectively. For participants scanned with [¹¹C]PBR28, MR scans were performed on a Siemens Magnetom Trio scanner, while PET scans were also performed on a Siemens Biograph 6, with list-mode data histogrammed into 26 frames (8 × 15 s, 3 × 60 s, 5 × 120 s, 5 × 300 s and 5 × 600 s) and reconstructed using FBP with a 5-mm Gaussian filter. For [¹⁸F]GE-180 scans, the tracer was injected 30 s after scan start time (two fewer frames in the reconstruction).

Image Analysis

PET images underwent frame-to-frame realignment and were coregistered with T1 MRI in PMOD (v3.6, PMOD Technologies Ltd., Switzerland). Coregistrations were quality checked manually. MRI was used to segment the brain into 83 regions using the Hammers atlas [19]. These regions

were inspected manually for overlap and edited where necessary to minimise spillover from large-vessel vascular activity. Respective smaller ROIs were then combined to create final bilateral ROIs as follows: frontal, temporal, parietal and occipital lobes (FL, TL, PL, OL), striatum, putamen, thalamus, cerebellum, corpus callosum, brainstem, whole brain (WB) and normal appearing white matter (NAWM). Lesions were defined semi-automatically on MRI using a local thresholding technique implemented in in-house software (BioMedIA group, Department of Computing, Imperial College London). T1, T2 fluid attenuated inversion recovery (FLAIR), double inversion recovery (DIR) and phase sensitive inversion recovery (PSIR) sequences were used to maximise sensitivity of lesion identification. All ROIs excluded lesions.

Kinetic Analysis

All kinetic analysis was performed in PMOD. Calibrated continuous and discrete blood data were corrected for decay and the parent fraction of tracer in plasma was calculated for each discrete sample. Plasma over blood (POB) ratios were calculated and the parent fraction of tracer in plasma fitted to a Watabe parent fraction model [20] of the form

$$f_{\text{parent}}(t) = f_p \cdot \left\{ \frac{1}{1 - \left(\frac{A^B}{u^B + C} \right)} \right\}, \text{ where } f_p \text{ is the free fraction of}$$

parent tracer and A , B , C and u are constants. This was multiplied with the continuous whole blood data to produce a metabolite-corrected arterial plasma input function. V_T was calculated from the unconstrained two-tissue compartment model as previously described [13, 14].

Calculating the Component of Non-Displaceable Binding

Three methods were used to determine the non-displaceable (V_{ND}) and displaceable (V_S) components of the total volume of distribution (V_T). Of these methods, two were independent: the occupancy plot (methods 1a and 1b) and the polymorphism plot (method 2).

Method 1a: Occupancy Plot with Individual V_{ND}

The occupancy plot is an adaptation of the Lassen plot described by Cunningham et al. [4]. Given that $V_T^{\text{baseline}} = V_S + V_{ND}$ (baseline condition) and $V_T^{\text{block}} = V_S (1 - \text{Occ}_{\text{drug}}) + V_{ND}$ (block condition), it follows that $V_T^{\text{baseline}} - V_T^{\text{block}} = \text{Occ}_{\text{drug}} \cdot (V_T^{\text{baseline}} - V_{ND})$. Thus, plotting V_T^{baseline} against $V_T^{\text{baseline}} - V_T^{\text{block}}$ allows derivation of V_{ND} (x-intercept) and the occupancy of XBD173 (slope). This method assumes that V_{ND} is the same at pre and post-block time points and that the fractional occupancy of XBD173

does not change across the brain. Method 1a plots these data for each individual participant.

Method 1b: Occupancy Plot with Constrained V_{ND}

In order to calculate a group V_{ND} , data from individual participants were plotted as described in method 1a, with the x -intercept forced to a best fit for all participants. This was done by constraining the x -intercept (V_{ND}) to be equal (for all participants) on a group level, using a linear regression implemented in Matlab (R2018a, The MathWorks, Inc., MA, USA).

Method 2: Polymorphism Plot

The polymorphism plot, described by Guo et al. [7], does not require pharmacological blockade. Instead, it relies upon the assumption that MABs express 50 % HAB and 50 % LAB binding sites [6, 9]. Thus, similarly to methods 1a and 1b, $V_T^{HAB} - V_T^{MAB} = \Delta(V_T^{HAB} - V_{ND})$, where Δ is a constant ($\frac{BP_{ND}^{HAB} - BP_{ND}^{MAB}}{BF_{ND}^{HAB}}$) relating to the non-displaceable binding potential, BP_{ND} , for HABs and LABs, respectively. Again, a plot of V_T^{HAB} against $V_T^{HAB} - V_T^{MAB}$ thus gives V_{ND} as the x -intercept.

Statistics

Linear regressions were generated in Matlab (R2018a, The MathWorks, Inc., MA, USA) and V_T and V_{ND} results are expressed as mean \pm standard deviation (SD). For each tracer, V_{TS} in different ROIs were compared using repeated measures one-way ANOVA with a Tukey test for multiple comparisons. Statistical tests were performed in GraphPad Prism (v7, GraphPad Software, Inc., San Diego, CA, USA).

Results

Demographics

The mean age of participants scanned with [¹⁸F]GE-180 was 46.8 ± 9.1 years, mean age of onset was 36.2 ± 12.8 years and EDSS ranged between 3.5 and 7.5. For [¹¹C]PBR28, mean age was 40.5 ± 9.0 years (unpaired t test: $p = 0.25$, not significant, ns, compared to [¹⁸F]GE-180), mean age of onset was 35.4 ± 6.2 years ($p = 0.78$, ns compared to [¹⁸F]GE-180) and EDSS ranged between 1 and 6.5 ($p = 0.13$, ns compared to [¹⁸F]GE-180). All participants had been treated with disease-modifying therapy. Participant demographics are summarised in Table 1.

Visual Assessment of PET Reveals Blockade of TSPO

Sixty- to 90-min sum PET images were generated for all participants. There was little obvious visual difference in sum PET images pre- and post-block (e.g., participants F and H, Figs. 1 and 2, right hand side) for participants scanned with [¹⁸F]GE-180 but a small decrease was evident with [¹¹C]PBR28. V_{TS} were then generated for all participants in all Hammers atlas ROIs and visualised as a heat map (left hand side, Figs. 1 and 2). In contrast to sum PET images, there were clear visual differences between pre- and post-block V_{TS} with both tracers.

[¹⁸F]GE-180 Binds Specifically to TSPO

Mean whole brain baseline V_T was 0.29 ± 0.17 ml/cm³ for [¹⁸F]GE-180 and 5.31 ± 1.53 for [¹¹C]PBR28. There were no significant differences in V_T between any ROIs for [¹⁸F]GE-180. For [¹¹C]PBR28, the putamen was elevated over NAWM ($p = 0.03$).

Blockade with XBD173 confirmed that both [¹⁸F]GE-180 and [¹¹C]PBR28 exhibit specific binding in the MS brain. Of the

Table 1.. Summary of participant demographics for those scanned with [¹⁸F]GE-180 and [¹¹C]PBR28

Tracer	Participant	HAB/MAB	Sex	Age/age at onset (years)	EDSS	Previous DMTs; current DMT
[¹⁸ F]GE-180	A	HAB	M	43/32	6.5	GA; GA
	B	MAB	M	53/36	4.0	IVIG, natalizumab; IVIG
	C	MAB	F	60/47	3.5	Alemtuzumab; alemtuzumab
	D	HAB	F	33/20	5.5	IB-1a/1b, natalizumab, alemtuzumab, AHSCT; natalizumab
	E	MAB	F	46/38	6.0	IB-1a, GA, fingolimod, natalizumab; alemtuzumab
	F	HAB	M	46/32	7.5	Natalizumab; AHSCT
[¹¹ C]PBR28	G	HAB	F	44/40	6.5	Natalizumab; natalizumab
	H	MAB	M	29/27	1.0	DF; DF
	I	MAB	F	39/30	6.5	Alemtuzumab, MSCT, natalizumab; MCTD
	J	MAB	F	56/44	4.0	Natalizumab, AHSCT, IB-1a; nil
	K	HAB	M	37/35.5	1.5	DF; nil
	L	HAB	M	38/36	1.5	DF; nil

HAB/MAB high/mixed affinity binder, EDSS (Kurtzke) expanded disability status scale, DMT disease modifying therapy, GA glatiramer acetate, IVIG intravenous immunoglobulin, IB interferon-beta, AHSCT autologous haematopoietic stem cell transplantation, DF dimethyl fumarate, MSC mesenchymal stem cell therapy, MCTD mixed connective tissue disease

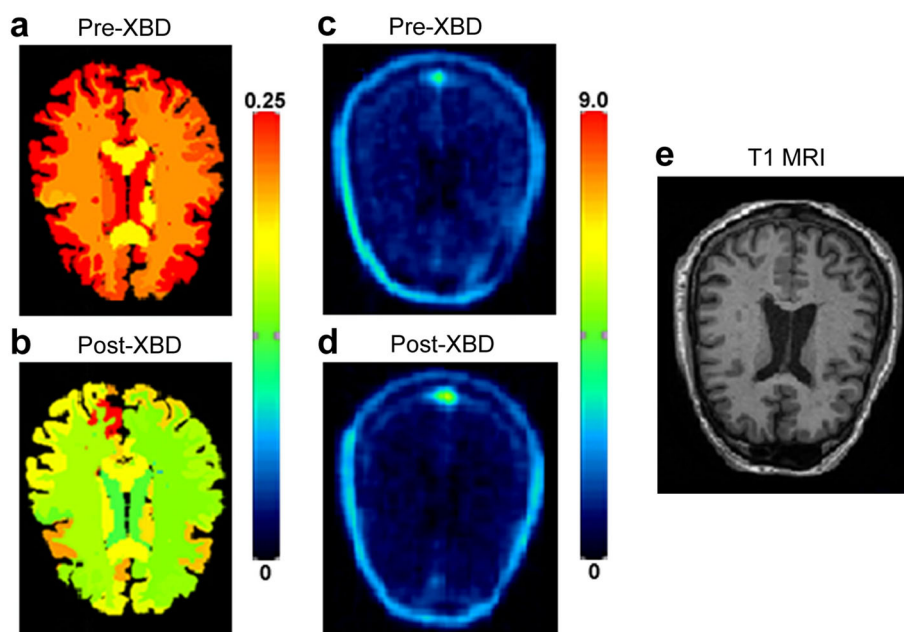


Fig. 1 Hammers atlas filled with V_T results in transverse view **a** pre- and **b** post-XBD173 administration, for participant F scanned with [¹⁸F]GE-180. V_T (ml/cm^3) for each region is mapped onto the participant's regional atlas in patient space. Sum 60–90 min PET images (kBq ml^{-1}) for the same subject in transverse view **c** pre- and **d** post-XBD173 administration. **e** T1 MRI for same subject.

12 participants, one displayed no measurable occupancy and was excluded from further analyses (participant K, HAB scanned with [¹¹C]PBR28). Mean whole brain baseline V_T for the remaining [¹¹C]PBR28 participants was $5.43 \pm 1.68 \text{ ml}/\text{cm}^3$.

Method 1a, the unconstrained occupancy plot, gave a mean V_{ND} of $0.18 \pm 0.05 \text{ ml}/\text{cm}^3$ for [¹⁸F]GE-180 and $3.65 \pm 1.79 \text{ ml}/\text{cm}^3$ for [¹¹C]PBR28. Method 1b, using an occupancy plot and constraining the x -intercept across participants, gave mean V_{ND}

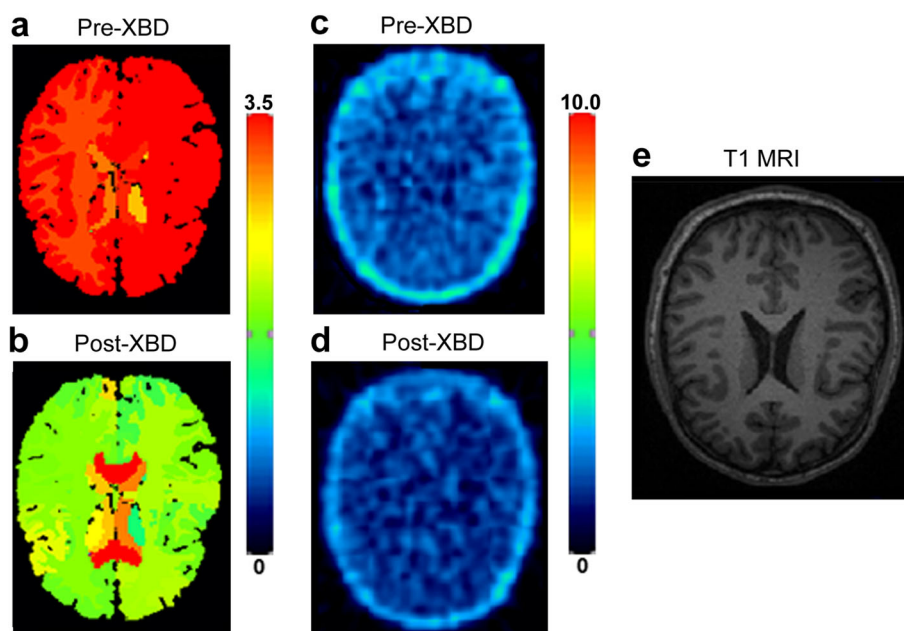


Fig. 2 Hammers atlas filled with V_T results in transverse view **a** pre- and **b** post-XBD173 administration, for participant H scanned with [¹¹C]PBR28. V_T (ml/cm^3) for each region is mapped onto the participant's regional atlas in patient space. Sum 60–90 min PET images (kBq ml^{-1}) for the same subject in transverse view **c** pre- and **d** post-XBD173 administration. **e** T1 MRI for same subject.

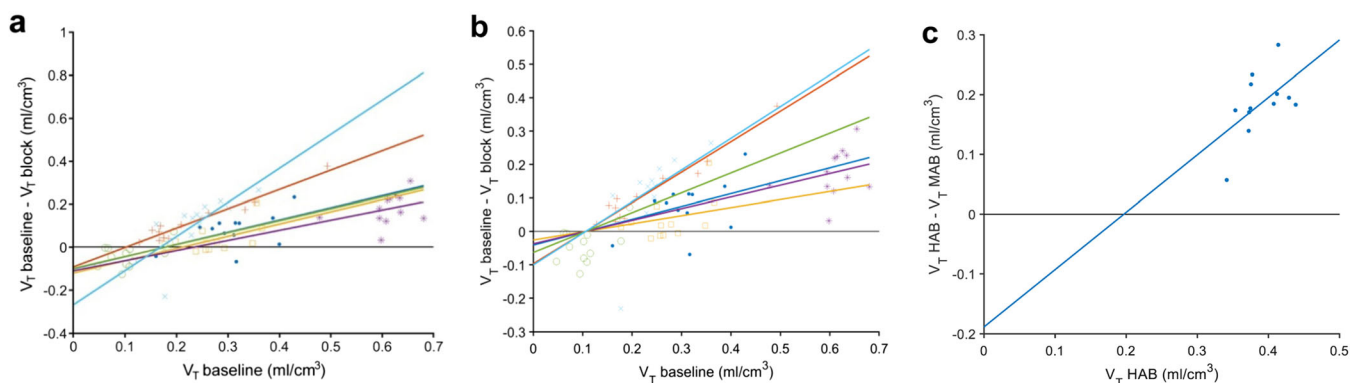


Fig. 3 **a** Individual linear regression with occupancy plot, **b** constrained x-intercept occupancy plot and **c** polymorphism plot, bottom for [¹⁸F]GE-180. V_{ND} is derived from the x-intercept. Different symbols indicate individual patients for **a** and **b**; each symbol represents a region of interest.

estimates of 0.11 and 3.81 ml/cm³ respectively. Method 2, using a polymorphism plot, produced V_{ND} estimates of 0.20 and 3.49 ml/cm³, respectively (Figs. 3 and 4). With V_{ND} estimates of 0.16 ± 0.05 ml/cm³ (mean of the three methods) for [¹⁸F]GE-180 and 3.65 ± 0.16 ml/cm³ for [¹¹C]PBR28 and mean baseline whole brain V_T of 0.29 and 5.43 ml/cm³, respectively, the specific binding ($V_S = V_T - V_{ND}$) accounted for 45 % of total V_T in the brain for [¹⁸F]GE-180 (57 % HABs; 20 % MABs) and 33 % for [¹¹C]PBR28 (37 % HABs; 25 % MABs). The reduction in uptake for both tracers post-XBD173 administration is further highlighted in Fig. 5, where a clear decrease in V_T in the majority of ROIs is observed. Furthermore, $BP_{ND} (= \frac{V_T}{V_{ND}} - 1)$ was used to calculate the mean HAB/MAB signal ratio for each tracer using these mean V_{ND} values. For [¹⁸F]GE-180, this was 5.45 ± 3.29 ($p < 0.01$), while for [¹¹C]PBR28, the HAB/MAB ratio was 3.21 ± 1.27 ($p < 0.01$).

Specific Binding to TSPO Is Ubiquitous in the MS Brain

For [¹⁸F]GE-180, V_S accounted for between 39 % (striatum) and 54 % (thalamus) of total binding in the selected ROIs

(mean \pm SD, 45 ± 5 %). For [¹¹C]PBR28, V_S accounted for between 6 % (striatum) and 43 % (brainstem) of total binding (29 ± 11 %). All other ROIs defined by the Hammers atlas, including the caudate and non-cortical GM, exhibited mean V_T between 0.25 and 0.56 ml/cm³ and between 3.99 and 7.39 ml/cm³, respectively. Thus, it follows that no ROIs were consistently devoid of specific TSPO binding, as measured by either tracer.

Discussion

This study was designed to quantify the non-specific binding (V_{ND}) of the TSPO PET tracers [¹⁸F]GE-180 and [¹¹C]PBR28 in people with MS. We found that V_{ND} accounts for, on average, 55 and 67 % of the total binding of [¹⁸F]GE-180 and [¹¹C]PBR28, respectively, indicating that the remaining 45 or 33 % are attributable to specific signal (V_S).

[¹⁸F]GE-180 has shown high signal-to-noise ratios in preclinical studies [10–12, 21, 22] but unexpectedly low brain penetration in human healthy controls [13–15]. Recent studies have demonstrated markedly increased uptake of [¹⁸F]GE-180 in people with glioblastoma [23] and in people

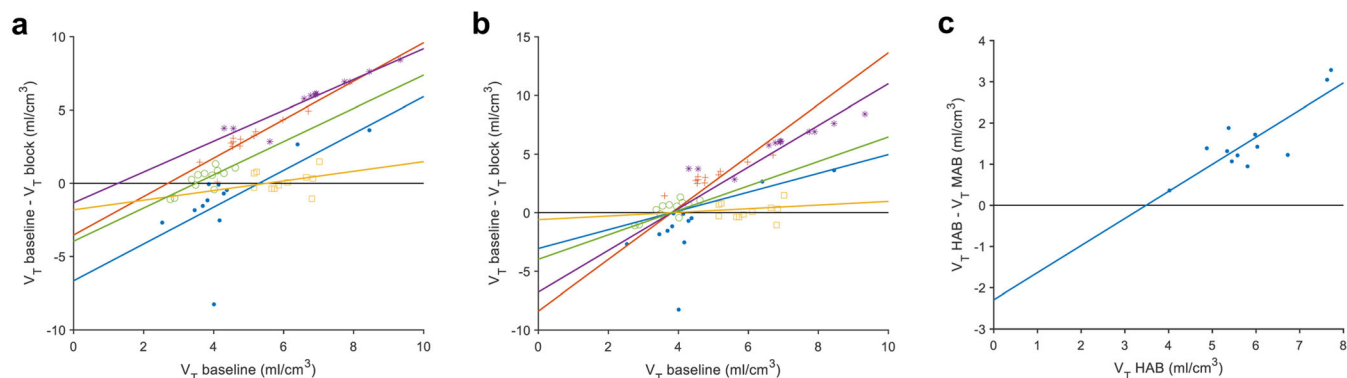


Fig. 4 **a** Individual linear regression with occupancy plot, **b** constrained x-intercept occupancy plot and **c** polymorphism plot, bottom for [¹¹C]PBR28. V_{ND} is derived from the x-intercept. Different symbols indicate individual patients for **a** and **b**; each symbol represents a region of interest.

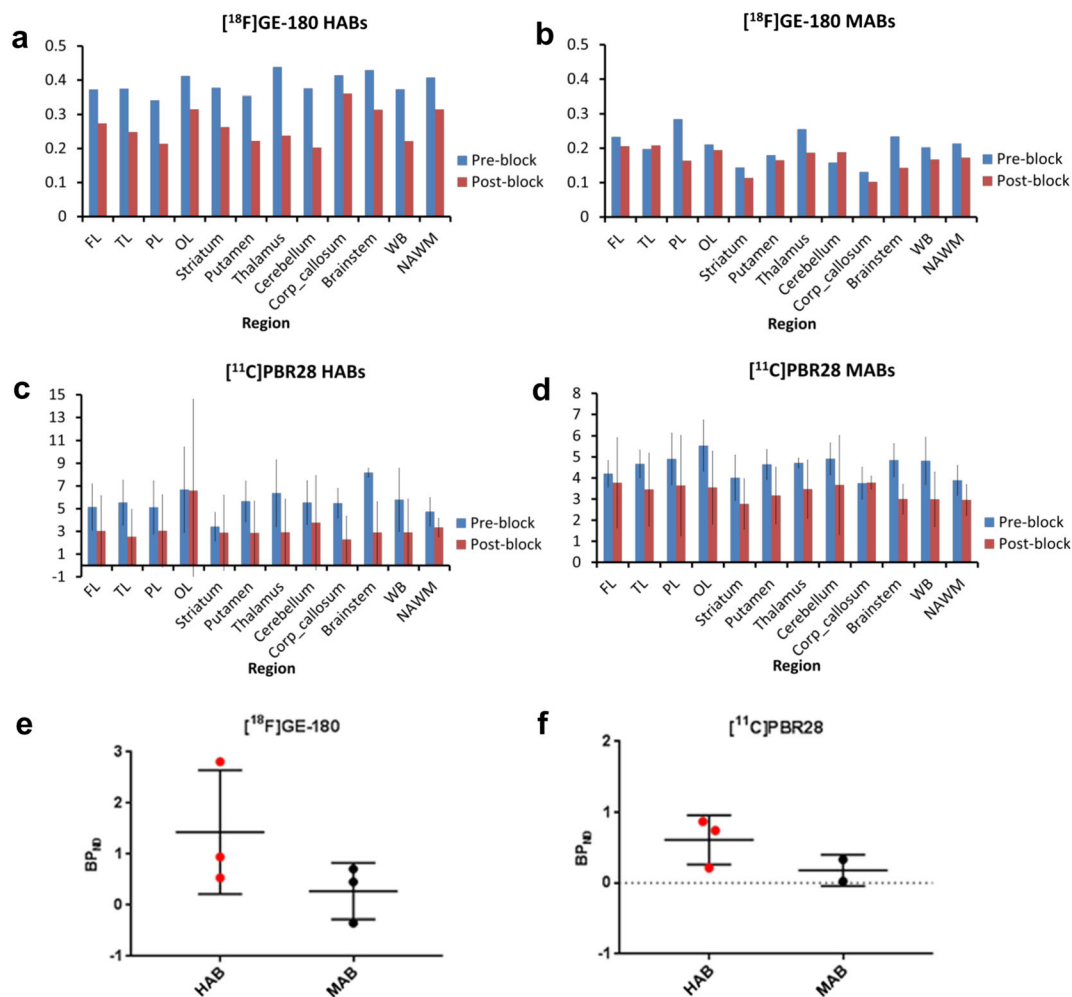


Fig. 5 Bar graph plots of average regional V_T pre- and post-blockade for HABs and MABs for **a** and **b**: [¹⁸F]GE-180; **c** and **d**: [¹¹C]PBR28. **e** and **f**: HAB vs. MAB group V_T estimates for each tracer ($n = 6$ [¹⁸F]GE-180; $n = 5$ [¹¹C]PBR28).

with relapsing-remitting MS [24], but questions remain as to whether this increase in signal represents specific binding or is merely due to non-specific signal in areas of blood–brain barrier breakdown. Another recent study which directly compared [¹⁸F]GE-180 with [¹¹C]PBR28 in healthy controls who were scanned with both tracers (morning and afternoon) found up to 20 times lower volumes of distribution with the former compared to the latter [15] as well as difficulties with [¹⁸F]GE-180 quantification. To our knowledge, ours is the first study assessing non-displaceable binding of [¹⁸F]GE-180 and comparing both tracers in disease cohorts. Our results argue that, despite low brain penetration [13, 14], [¹⁸F]GE-180 does exhibit a specific signal in the MS brain and hence could be useful in conditions with pathologically increased levels of TSPO. We also performed gadolinium contrast-enhancing MRI in the cohort of participants scanned with [¹⁸F]GE-180 and observed no contrast enhancement (in lesion areas or otherwise), suggesting no extensive BBB breakdown. Although this observation does not exclude the possibility of micro-BBB breakdown, which could allow passage of [¹⁸F]GE-180 molecules, but not the

larger gadolinium molecules, through the disrupted area, the finding does concur with that of Vomacka et al. [25]. The authors of this study also comment that (in their previous study [23]) areas with contrast enhancement in MR did not always correlate with increased [¹⁸F]GE-180 signal, indicating that signal increases in PET are likely to be related to TSPO expression rather than exclusively BBB breakdown. The results also have broader implications on how novel tracers should be validated and compared. While high absolute V_T s are preferable in a tracer, it is crucial to understand what proportion of V_T is driven by V_{ND} . This can be achieved using a blocking study, which, given the lack of an appropriate receptor-free reference region in the brain, we suggest should be undertaken for all TSPO tracers undergoing clinical development.

Although the occupancy plot has been more commonly used in V_{ND} quantification [4], an alternative approach, relevant for TSPO tracers which are susceptible to the rs6971 SNP, is to create a polymorphism plot, which does not require pharmacological blockade and relies only on the assumption of equal expression of HAB and LAB sites. Our

V_{ND} results from both methods (including free and fixed-intercept occupancy plots) were in good agreement for both tracers, giving an average V_{ND} of 0.16 ± 0.05 ml/cm³ for [¹⁸F]GE-180 and 3.65 ± 0.16 ml/cm³ for [¹¹C]PBR28. In this study, we also demonstrate that V_T is consistently greater than V_{ND} for both [¹⁸F]GE-180 and [¹¹C]PBR28; in other words, no ROIs were devoid of specific TSPO binding. This finding fits with previous observations that reference tissue approaches may not be appropriate in TSPO PET studies [6].

[¹¹C]PBR28 has been validated with blocking experiments prior to our study, both in healthy controls [6, 26] and in a disease cohort [27]. [¹¹C]PBR28 is generally accepted as an effective TSPO tracer *in vivo* [28–32] although exhibits counterintuitively decreased V_T in subjects with neuroinflammation [29]. In Owen et al. [6], the V_{ND} of [¹¹C]PBR28 was 1.98 ml/cm³ (~50 % of V_T), while Fujita et al. [26] reported an average V_T of 4.3 ml/cm³ (in HABs) and a BP_{ND} of 1.2, giving a very similar V_{ND} of 1.98 ml/cm³ (~45 % of V_T). In our study, V_{ND} for [¹¹C]PBR28 was 3.65. It is possible that this is a disease-specific difference, given that both the former studies were performed in healthy subjects; however, the sample size in our study was also small and the estimation of V_{ND} may therefore be subject to some biological variability. Nevertheless, the proportion of non-specific binding for [¹⁸F]GE-180 is comparable to or even lower than that of [¹¹C]PBR28 ($V_{ND} \sim 55$ vs. ~69 %, respectively), although absolute V_{TS} are lower [6, 27]. This result further indicates that [¹⁸F]GE-180 is able to identify specific TSPO signal in the MS brain, in spite of low brain penetration. We also report respective HAB and MAB V_S of 57 and 20 % for [¹⁸F]GE-180 and 37 and 25 % for [¹¹C]PBR28, although the group numbers ($n=3$ for both [¹⁸F]GE-180 groups and [¹¹C]PBR28 HABs, $n=2$ for [¹¹C]PBR28 MABs) are too small to draw firm conclusions.

As has been pointed out previously, the brain penetration of [¹⁸F]GE-180 is very low in humans [13–15]. Our findings also showed low values of V_T and K_1 , indicating low extraction of the tracer across the blood–brain barrier ($K_1 \sim 0.003$ vs. 0.2 ml/cm³/min for [¹¹C]PBR28; *i.e.*, ~60× lower). Zanotti-Fregonara and colleagues also noted difficulty in kinetic model fitting of [¹⁸F]GE-180 data using the standard two-tissue compartment model with free blood volume parameter, which we used [15]. Here, however, we were able to fit the large majority of regions well, with R^2 comparable to those seen with [¹¹C]PBR28 ($R^2 \sim 0.8$) and standard errors on V_T estimates <20 % for both tracers. It is possible that this is due to the larger, less noisy ROIs selected for analysis in our study compared to those used by Zanotti-Fregonara and colleagues. Also to be considered is the fact that our study involved (six) participants with MS, compared to the four healthy controls and single participant with amyotrophic lateral sclerosis in the other study, which may have resulted in altered binding kinetics due to disease-specific pathology. Although a methodology considering large ROIs in a disease such as MS, with focal lesion-based pathology, may seem to limit the usefulness of a tracer,

there is evidence that there is a global effect on TSPO PET signal in regions such as NAWM and normal appearing grey matter (see [33] for review), suggesting that [¹⁸F]GE-180 need not be excluded from use based on this fact. Many recent studies using [¹¹C]PBR28 (and other tracers) have elected to use the 2TCM-1K kinetic model [34], which incorporates a parameter representing the endothelial fraction of binding of a TSPO tracer, for quantification [29]. The 2TCM-1K has been used with [¹⁸F]GE-180 data [13] and has not shown a substantial advantage in terms of parsimony criteria (Akaike Information Criteria, AIC) compared to the 2TCM. Furthermore, [¹¹C]PBR28 datasets are often still analysed using the 2TCM, primarily for comparison with data from other tracers [15, 35, 36]. We also found good fits to [¹¹C]PBR28 data with the 2TCM; thus, here, we elected to use this model to analyse data from both tracers.

The *in vitro* HAB/LAB ratio of binding affinity for [¹¹C]PBR28 has been observed to be approximately 1:50 [9], while for [¹⁸F]GE-180, this ratio is between 1:5 and 1:15 (personal communication, DRO, WT). *In vivo*, [¹¹C]PBR28-scanned MABs express approximately half the signal compared to HABs [6]. The slope of the polymorphism plot is equivalent to $\frac{BP_{ND}^{HAB} - BP_{ND}^{MAB}}{BP_{ND}^{HAB}}$. For [¹⁸F]GE-180, our equivalent *in vivo* HAB/MAB ratio was found to be 5.43 ± 3.27 and the average slope was thus expected to be approximately 0.8, while for [¹¹C]PBR28, these values were 3.21 ± 1.27 and 0.7. Our results for the slopes of the polymorphism plots were 0.96 and 0.67 respectively and thus fell within one standard deviation of the predicted values. Previous studies using [¹⁸F]GE-180 have been unable to detect consistent differences in tracer signal between HABs and MABs [13, 14, 24], indicating that brain penetration of the tracer is low, except where BBB breakdown may be present [24]. Contrary to these results, in our study, HABs exhibited approximately twice the total volume of distribution of MABs in selected ROIs at baseline. It is likely that the difference in our study is driven primarily by one HAB with particularly high signal (participant D) and one MAB with particularly low signal (participant E). Clearly there is considerable variability in population V_T and with the small sample size in our study ($n=6$), we are unable to validate our findings with statistical tests. In addition, the difference in scan timing between the first and second (post-XBD173) scan varied for each tracer (half a day for [¹¹C]PBR28 and 1 week for [¹⁸F]GE-180), which itself may have introduced some variability in PET signal. Thus, we suggest continuing binding status stratification of participants in future studies, where larger data pools may enable more reliable HAB/MAB binding ratio estimates.

Several caveats exist in this study. Firstly, the occupancy of XBD173 in the two cohorts (slopes in the occupancy plots) varied between 24 and 95 % (fixed-intercept plot) for [¹⁸F]GE-180 and 16 and 220 % for [¹¹C]PBR28. Clearly, the occupancy of XBD173 cannot

exceed 100 %, and indeed, the dose administered was pre-calculated to give an expected approximate 75 % occupancy, allowing for participant weights and considering the dose-occupancy relationship described by Owen et al. [6] for [¹¹C]PBR28. Of course, it should also be noted that these values were obtained from the fixed-intercept occupancy plot; for the free intercept plot, occupancies were within one standard deviation of the expected value. This point again highlights the large variability across cohorts and the fact that averaging results across participants, even within the same disease population, may not be a suitable approach. In addition, one participant scanned with [¹¹C]PBR28 exhibited no substantial occupancy and was excluded from further analysis. This large inter-individual variability in occupancy was also seen in previous XBD173 blocking studies [6, 27], reflected in the variability in total signal reduction (V_T) between pre and post-block scans. Whether driven by biological variability or experimental noise, these results provide evidence that V_{ND} cannot necessarily be assumed to be the same across regions and a population. If there is indeed a biological spectrum of V_{ND} between individuals, this raises the interesting possibility that blocking scans should be included for all participants in all TSPO PET studies to optimally quantify V_S . This would have broad repercussions on TSPO PET study design, including cost, radiation exposure and participant discomfort. All neuro-PET tracers are, of course, better able to penetrate brain tissue when the BBB is disrupted. In the case of [¹⁸F]GE-180, which exhibits low penetration of the healthy BBB, this is particularly relevant. Although our cohorts were selected due to their clinically low or ‘inactive’ MRI, and although we investigated only lesion-free ROIs, we only performed contrast enhanced MRI to estimate BBB integrity in the [¹⁸F]GE-180 cohort, and no measure of micro-BBB disruption was performed. Lastly, although this study was performed in a cohort of people with MS, we have not investigated how V_T differs in MS lesions or how it correlates with clinical outcomes. This study was not powered to address these questions, since participants were not burdened with large lesion loads. Instead, these questions will be explored in follow-up studies.

Conclusion

In summary, pharmacological blockade with XBD173 demonstrates, for the first time *in vivo*, that [¹⁸F]GE-180 does bind specifically to TSPO in normal appearing white and grey matter, to an extent that is highly comparable to [¹¹C]PBR28, in spite of the low extraction fraction of the former.

Acknowledgements. The authors wish to thank Dr. William Trigg (formerly GE Healthcare), Dr. Christopher Buckley and Ms. Joanne Stevens (GE Healthcare) and Professor Federico Turkheimer (King’s College London) for their valuable advice during the analysis and write-up of this study.

Funding Information. This [¹⁸F]GE-180 arm of the study was funded by grants from GE Healthcare, FastForward and the MSTC, awarded to the Imperial College Trust. The [¹¹C]PBR28 arm of the study was funded by an Imperial College BRC IMPETUS 2014 grant.

Compliance with Ethical Standards

Conflict of Interest

SS, RN and JR have received funding from GE Healthcare. JR is a current employee of the MHRA; work herein was completed while JR was employed by Imperial College.

PAM declares honoraria for speaking and travel support from Bayer, Biogen, Merck Serono and Novartis.

DJB holds consultancies with GE Healthcare and Biogen.

RG is an employee of Invicro, Ltd.

All other authors have no disclosures.

Open Access This article is distributed under the terms of the Creative Commons Attribution 4.0 International License (<http://creativecommons.org/licenses/by/4.0/>), which permits unrestricted use, distribution, and reproduction in any medium, provided you give appropriate credit to the original author(s) and the source, provide a link to the Creative Commons license, and indicate if changes were made.

Publisher’s Note Springer Nature remains neutral with regard to jurisdictional claims in published maps and institutional affiliations.

References

- Rupprecht R, Papadopoulos V, Rammes G, Baghai TC, Fan J, Akula N, Groyer G, Adams D, Schumacher M et al (2010) Translocator protein (18 kDa) (TSPO) as a therapeutic target for neurological and psychiatric disorders. *Nat Rev Drug Discov* 9:971–988
- Owen DR, Yeo AJ, Gunn RN, Song K, Wadsworth G, Lewis A, Rhodes C, Pulford DJ, Bennacef I, Parker CA, StJean PL, Cardon LR, Mooser VE, Matthews PM, Rabiner EA, Rubio JP et al (2012) An 18-kDa translocator protein (TSPO) polymorphism explains differences in binding affinity of the PET radioligand PBR28. *J Cereb Blood Flow Metab* 32:1–5
- Turkheimer FE, Rizzo G, Bloomfield PS, Howes O, Zanotti-Fregonara P, Bertoldo A, Veronese M et al (2015) The methodology of TSPO imaging with positron emission tomography. *Biochem Soc Trans* 43:586–592
- Cunningham VJ, Rabiner EA, Slifstein M, Laruelle M, Gunn RN et al (2010) Measuring drug occupancy in the absence of a reference region: the Lassen plot re-visited. *J Cereb Blood Flow Metab* 30:46–50
- Lassen NA, Bartenstein PA, Lammertsma AA, Prevett MC, Turton DR, Luthra SK, Osman S, Bloomfield PM, Jones T, Patsalos PN, O’Connell MT, Duncan JS, Andersen JV et al (1995) Benzodiazepine receptor quantification *in vivo* in humans using [¹¹C] flumazenil and PET: application of the steady-state principle. *J Cereb Blood Flow Metab* 15:152–165
- Owen DR, Guo Q, Kalk NJ, Colasanti A, Kalogiannopoulou D, Dimber R, Lewis YL, Libri V, Barletta J, Ramada-Magalhaes J, Kamalakaran A, Nutt DJ, Passchier J, Matthews PM, Gunn RN, Rabiner EA et al (2014) Determination of [¹¹C]PBR28 binding potential *in vivo*: a first human TSPO blocking study. *J Cereb Blood Flow Metab* 34:989–994
- Guo Q, Colasanti A, Owen DR, Onega M, Kamalakaran A, Bennacef I, Matthews PM, Rabiner EA, Turkheimer FE, Gunn RN et al (2013) Quantification of the specific translocator protein signal of ¹⁸F-PBR111 in healthy humans: a genetic polymorphism effect on *in vivo* binding. *J Nucl Med* 54:1915–1923
- Guo Q, Owen DR, Rabiner EA, Turkheimer FE, Gunn RN (2014) A graphical method to compare the *in vivo* binding potential of PET radioligands in the absence of a reference region: application to

- [¹¹C]PBR28 and [¹⁸F]PBR111 for TSPO imaging. *J Cereb Blood Flow Metab* 34:1162–1168
9. Owen DR, Howell OW, Tang SP, Wells LA, Bennacef I, Bergstrom M, Gunn RN, Rabiner EA, Wilkins MR, Reynolds R, Matthews PM, Parker CA et al (2010) Two binding sites for [3H]PBR28 in human brain: implications for TSPO PET imaging of neuroinflammation. *J Cereb Blood Flow Metab* 30:1608–1618
 10. Boutin H, Murray K, Pradillo J, Maroy R, Smigova A, Gerhard A, Jones PA, Trigg W et al (2015) ¹⁸F-GE-180: a novel TSPO radiotracer compared to ¹¹C-R-PK11195 in a preclinical model of stroke. *Eur J Nucl Med Mol Imaging* 42:503–511
 11. Dickens AM, Vainio S, Marjamaki P, Johansson J, Lehtiniemi P, Rokka J, Rinne J, Solin O, Haaparanta-Solin M, Jones PA, Trigg W, Anthony DC, Airas L et al (2014) Detection of microglial activation in an acute model of neuroinflammation using PET and radiotracers C-11-(R)-PK11195 and F-18-GE-180. *J Nucl Med* 55:466–472
 12. James ML, Belichenko NP, Shuhendler AJ, Hoehne A, Andrews LE, Condon C, Nguyen TVV, Reiser V, Jones P, Trigg W, Rao J, Gambhir SS, Longo FM et al (2017) [¹⁸F]GE-180 PET detects reduced microglia activation after LM11A-31 therapy in a mouse model of Alzheimer's disease. *Theranostics* 7:1422–1436
 13. Fan Z, Calsolaro V, Atkinson RA, Femminella GD, Waldman A, Buckley C, Trigg W, Brooks DJ, Hinz R, Edison P et al (2016) Flutriclamide (¹⁸F-GE180) PET: first-in-human PET study of novel third-generation in vivo marker of human translocator protein. *J Nucl Med* 57:1753–1759
 14. Feeney C, Scott G, Raffel J, Roberts S, Coello C, Jolly A, Searle G, Goldstone AP, Brooks DJ, Nicholas RS, Trigg W, Gunn RN, Sharp DJ et al (2016) Kinetic analysis of the translocator protein positron emission tomography ligand [¹⁸F]GE-180 in the human brain. *Eur J Nucl Med Mol Imaging* 43:2201–2210
 15. Zanotti-Fregonara P, Pascual B, Rizzo G et al (2018) Head-to-head comparison of ¹¹C-PBR28 and ¹⁸F-GE180 for the quantification of TSPO in the human brain. In *J Nucl Med* 59(8):1260–1266
 16. Owen DRJ, Gunn RN, Rabiner EA, Bennacef I, Fujita M, Kreisl WC, Innis RB, Pike VW, Reynolds R, Matthews PM, Parker CA et al (2011) Mixed-affinity binding in humans with 18-kDa translocator protein ligands. *J Nucl Med* 52:24–32
 17. Kurtzke JF (1983) Rating neurologic impairment in multiple sclerosis: an expanded disability status scale (EDSS). *Neurology* 33:1444–1452
 18. Wadsworth H, Jones PA, Chau WF, Durrant C, Fouladi N, Passmore J, O'Shea D, Wynn D, Morisson-Iveson V, Ewan A, Thaning M, Mantzilas D, Gausemel I, Khan I, Black A, Avory M, Trigg W et al (2012) [¹⁸F]GE-180: a novel fluorine-18 labelled PET tracer for imaging translocator protein 18 kDa (TSPO). *Bioorg Med Chem Lett* 22:1308–1313
 19. Hammers A, Allom R, Free SL et al (2002) Three-dimensional probabilistic atlas of the human brain. *Neuroimage* 16:S86–S86
 20. Watabe H, Channing MA, Der MG et al (2000) Kinetic analysis of the 5-HT_{2A} ligand [¹¹C] MDL 100,907. *J Cereb Blood Flow Metab* 20:899–909
 21. Sridharan S, Lepelletier FX, Trigg W, Banister S, Reekie T, Kassiou M, Gerhard A, Hinz R, Boutin H et al (2017) Comparative evaluation of three TSPO PET radiotracers in a LPS-induced model of mild neuroinflammation in rats. *Mol Imaging Biol* 19:77–89
 22. Russmann V, Brendel M, Mille E, Helm-Vicidomini A, Beck R, Günther L, Lindner S, Rominger A, Keck M, Salvamoser JD, Albert NL, Bartenstein P, Potschka H et al (2017) Identification of brain regions predicting epileptogenesis by serial [¹⁸F]GE-180 positron emission tomography imaging of neuroinflammation in a rat model of temporal lobe epilepsy. *Neuroimage Clin* 15:35–44
 23. Albert NL, Unterrainer M, Fleischmann DF, Lindner S, Vettermann F, Brunegraf A, Vomacka L, Brendel M, Wenter V, Wetzel C, Rupprecht R, Tonn JC, Belka C, Bartenstein P, Niyazi M et al (2017) TSPO PET for glioma imaging using the novel ligand ¹⁸F-GE-180: first results in patients with glioblastoma. *Eur J Nucl Med Mol Imaging* 44:2230–2238
 24. Unterrainer M, Mahler C, Vomacka L, Lindner S, Havla J, Brendel M, Böning G, Ertl-Wagner B, Kümpfel T, Milenkovic VM, Rupprecht R, Kerscheneister M, Bartenstein P, Albert NL et al (2018) TSPO PET with [(18)F]GE-180 sensitively detects focal neuroinflammation in patients with relapsing-remitting multiple sclerosis. *Eur J Nucl Med Mol Imaging* 45:1423–1431
 25. Vomacka L, Albert NL, Lindner S, Unterrainer M, Mahler C, Brendel M, Ermoschkin L, Gosewisch A, Brunegraf A, Buckley C, Kümpfel T, Rupprecht R, Ziegler S, Kerscheneister M, Bartenstein P, Böning G et al (2017) TSPO imaging using the novel PET ligand [¹⁸F]GE-180: quantification approaches in patients with multiple sclerosis. *EJNMMI Res* 7:89
 26. Fujita M, Kobayashi M, Ikawa M, Gunn RN, Rabiner EA, Owen DR, Zoghbi SS, Haskali MB, Telu S, Pike VW, Innis RB et al (2017) Comparison of four ¹¹C-labeled PET ligands to quantify translocator protein 18 kDa (TSPO) in human brain: (R)-PK11195, PBR28, DPA-713, and ER176-based on recent publications that measured specific-to-non-displaceable ratios. *EJNMMI Res* 7:84
 27. Veronese M, Reis Marques T, Bloomfield PS, Rizzo G, Singh N, Jones D, Agushi E, Mosses D, Bertoldo A, Howes O, Roncaroli F, Turkheimer FE et al (2018) Kinetic modelling of [¹¹C]PBR28 for 18 kDa translocator protein PET data: a validation study of vascular modelling in the brain using XBD173 and tissue analysis. *J Cereb Blood Flow Metab* 38:1227–1242
 28. Albrecht D, Shcherbinin S, Wooten D et al (2016) Occipital lobe as a pseudo-reference region for [¹¹C]PBR28 PET imaging: validation in chronic pain and amyotrophic lateral sclerosis cohorts. *J Nucl Med* 57:1814
 29. Bloomfield PS, Selvaraj S, Veronese M, Rizzo G, Bertoldo A, Owen DR, Bloomfield MAP, Bonoldi I, Kalk N, Turkheimer F, McGuire P, de Paola V, Howes OD et al (2016) Microglial activity in people at ultra high risk of psychosis and in schizophrenia: an [¹¹C]PBR28 PET brain imaging study. *Am J Psychiatry* 173:44–52
 30. Datta G, Colasanti A, Kalk N, Owen D, Scott G, Rabiner EA, Gunn RN, Lingford-Hughes A, Malik O, Ciccarelli O, Nicholas R, Nei L, Battaglini M, Stefano ND, Matthews PM et al (2017) ¹¹C-PBR28 and ¹⁸F-PBR111 detect white matter inflammatory heterogeneity in multiple sclerosis. *J Nucl Med* 58:1477–1482
 31. Kreisl WC, Fujita M, Fujimura Y, Kimura N, Jenko KJ, Kannan P, Hong J, Morse CL, Zoghbi SS, Gladding RL, Jacobson S, Oh U, Pike VW, Innis RB et al (2010) Comparison of [¹¹C]-(R)-PK 11195 and [¹¹C]PBR28, two radioligands for translocator protein (18 kDa) in human and monkey: implications for positron emission tomographic imaging of this inflammation biomarker. *Neuroimage* 49:2924–2932
 32. Park E, Gallezot JD, Delgadillo A, Liu S, Planeta B, Lin SF, O'Connor KC, Lim K, Lee JY, Chastre A, Chen MK, Seneca N, Leppert D, Huang Y, Carson RE, Pelletier D et al (2015) ¹¹C-PBR28 imaging in multiple sclerosis patients and healthy controls: test-retest reproducibility and focal visualization of active white matter areas. *Eur J Nucl Med Mol Imaging* 42:1081–1092
 33. Airas L, Nylund M, Rissanen E (2018) Evaluation of microglial activation in multiple sclerosis patients using positron emission tomography. *Front Neurol* 9:181
 34. Rizzo G, Veronese M, Tonietto M, Zanotti-Fregonara P, Turkheimer FE, Bertoldo A et al (2014) Kinetic modeling without accounting for the vascular component impairs the quantification of [¹¹C]PBR28 brain PET data. *J Cereb Blood Flow Metab* 34:1060–1069
 35. Collste K, Forsberg A, Varrone A, Amini N, Aeinband S, Yakushev I, Halldin C, Farde L, Cervenka S et al (2016) Test-retest reproducibility of [C-11]PBR28 binding to TSPO in healthy control subjects. *Eur J Nucl Med Mol Imaging* 43:173–183
 36. Collste K, Plaven-Sigra P, Fatouros-Bergman H et al (2017) Lower levels of the glial cell marker TSPO in drug-naïve first-episode psychosis patients as measured using PET and [¹¹C]PBR28. *Mol Psychiatry* 22:850–856